

DR. DANIEL E. FALVEY (Orcid ID : 0000-0002-2185-502X)

Article type : Special Issue Research Article

## **SPECIAL ISSUE RESEARCH ARTICLE**

# **Visible-Light Photocatalytic Oxidation of DMSO for RAFT Polymerization<sup>†</sup>**

Matthew D. Thum, Donald Hong, Andrea N. Zeppuhar, and Daniel E. Falvey\*

University of Maryland, College Park

Department of Chemistry and Biochemistry, MD (USA) 20942

\*Corresponding author e-mail: Falvey@umd.edu (Daniel E. Falvey)

<sup>†</sup>This article is part of a Special Issue celebrating the career of Dr. Edward Clennan

This article has been accepted for publication and undergone full peer review but has not been through the copyediting, typesetting, pagination and proofreading process, which may lead to differences between this version and the [Version of Record](#). Please cite this article as [doi: 10.1111/PHP.13468](https://doi.org/10.1111/PHP.13468)

This article is protected by copyright. All rights reserved

## ABSTRACT

The solvent is an important, yet often forgotten part of a reaction mechanism. Many photochemical polymerizations are carried out using dimethyl sulfoxide (DMSO) as a way to promote the solubility of both the reactants and products, but its reactivity is rarely considered when initiation mechanisms are proposed. Herein, the oxidation of DMSO by an excited state quinone is used to form initiating radicals resulting in the polymerization of methacrylate monomers, and the polymerization can be controlled with the addition of a chain transfer agent. This process leads to the formation of polymers with narrow molecular weight distribution and the polymerization is able to be carried out in the presence of oxygen. A visible light absorbing substituted anthraquinone is synthesized and nanosecond transient absorption spectroscopy is used to monitor the intermediates involved in the initiation mechanism. Photoproduct analysis indicates formation of methyl radicals as a result of DMSO oxidation. Furthermore, we show that the solvent outcompetes the chain transfer agent for interacting with the excited-state anthraquinone. These observations have a broad impact on photoinduced polymerizations performed in DMSO as many photocatalysts are strong oxidants in the excited state and are capable of reacting with the solvent. Therefore, the role of the solvent needs to be more carefully considered when proposing mechanisms for photoinduced polymerizations in DMSO.

## INTRODUCTION

Photomediated controlled radical polymerization is a popular method for preparing well-defined polymers due to its mild reaction conditions and the ability to provide the overall process of the reaction with spatial and temporal specificity. The ability of light to switch the polymerization process “on” and “off” is advantageous in the manufacturing of polymers with exact control over the molecular properties of the final product. One area in which this approach has been adopted wholeheartedly is reversible addition-fragmentation chain transfer (RAFT) polymerization. Light has been used multiple ways to initiate RAFT polymerization.<sup>1–6</sup> Traditionally, RAFT polymerization is carried out under direct UV irradiation via a photoiniferter method. In this case, a dithioester, or related species, is directly irradiated which results in C-S homolysis and allows the RAFT agent to serve as both chain transfer agent (CTA) and photoinitiator.<sup>7–14</sup> Since these processes require only monomer and CTA, photoiniferter methods are valued for their simplicity. However, photodissociation of the CTA generally requires UV wavelengths which can result in unwanted degradation during photolysis, reducing end group fidelity and limiting high conversions.<sup>13–15</sup> Furthermore, photoiniferter processes are usually incompatible with molecular oxygen, limiting their potential applications.

An alternative approach, described by Hawker, Boyer, and others, uses photosensitizers (or photoredox catalysts) to trigger the initiation step.<sup>16–20</sup> Photocatalysts are strong excited state oxidants or reductants which are designed to activate CTAs through either excited-state energy transfer, or mediated one-electron transfer processes. The general photocatalytic RAFT scheme assumes that the photocatalyst generates radicals through interaction with the CTA, either via direct reduction, or via homolysis due to energy transfer.<sup>21–23</sup> In the photoinduced electron transfer (PET) mechanism, the excited state photocatalyst reacts either with the CTA directly, resulting in reduction of the CTA and subsequent radical formation, or acts a mediator by first reacting with a sacrificial electron donor, such as a tertiary amine, followed by reduction of the CTA. Photocatalytic RAFT is valued because it can provide access to a broad spectrum of irradiation wavelengths.<sup>20</sup> For example, the Boyer group demonstrated the use of visible light absorbing dyes such as Eosin Y and chlorophyll A in the

polymerization of methyl acrylate monomers and the Fors group described controlled cationic polymerization of vinyl ethers initiated by the photoreduction of dithiolates by oxidizing pyrilium salts.<sup>24–26</sup> The photocatalytic approach is attractive as it generally results in less undesired degradation of the products, however, these systems are more complex, often requiring photocatalyst and ground state donor in addition to monomer and CTA.

Recently, Corrigan et al. developed a method in which metal phthalocyanines, activated by NIR irradiation, were used in the controlled polymerization of acrylate monomers.<sup>27</sup> Interestingly, the initiation step did not involve photoreduction of the RAFT agent, rather, the excited photocatalyst reacts with the solvent, N-methyl-2-pyrrolidone, to generate initiating radicals. This approach eliminates the need for an additional ground-state donor or cosensitizer.

Dimethylsulfoxide (DMSO) is a widely used solvent for polymerization reactions in general, and photo-RAFT polymerization in particular. While it is normally believed to function as an inert medium, some reports show that DMSO can produce radicals under highly oxidizing conditions (Scheme 1), and in the presence of oxygen and a strong base.<sup>28</sup> The oxidation potential for DMSO has been estimated to be of +1.56 to +1.76 V (vs SCE).<sup>29</sup> Furthermore, on the basis of pulse radiolysis kinetics, it was inferred that one electron oxidation DMSO in the presence of water leads to formation of sulfinic acid along with highly reactive methyl radicals.<sup>30–32</sup> This was later adapted for the free radical methylation of 2'-deoxyguanosine.<sup>33</sup>

<Scheme 1>

The study described herein was undertaken to determine if a similar DMSO oxidation reaction would be present in a photo-RAFT process, and how that would affect the initiation mechanism(s). Excited-state quinones have been used extensively as excited state oxidants, as well the source for mediated electron transfer from a donor to an acceptor.<sup>34–40</sup> Most notably, the triplet state of most quinones is formed with high efficiency and photoreduction via hydrogen atom abstraction, or electron transfer are common.<sup>37</sup> Of particular relevance is an earlier laser flash photolysis study by Görner which established that triplet state 9,10-anthraquinone derivatives react rapidly with DMSO through one electron transfer.<sup>41</sup> For this reason, we examined a visible light absorbing anthraquinone derivative

(AQ-1, Fig. 1) and investigated its ability to promote photocatalytic RAFT through radical generation using the solvent, DMSO. Product analysis, laser flash photolysis (LFP), and chemical trapping experiments demonstrate that this approach provides visible light driven controlled radical polymerization through the interaction of the excited-state photosensitizer with the solvent which outcompetes reactions with the RAFT agent contrary to more conventional photo-RAFT processes.

<Figure 1>

## MATERIALS AND METHODS

**General Procedures:** All  $^1\text{H}$  and  $^{13}\text{C}$  NMR were obtained on a Bruker 400 MHz spectrometer.

Chemical shifts ( $\delta$ ) are reported in parts per million (ppm). Ultraviolet-visible (UV/Vis) spectra were recorded on a Shimadzu UV-1800 spectrometer using UVProbe 2.43 software. Samples were scanned from 200 to 600 nm using a fast scanning speed and a sampling interval of 1.0 nm. Mass spectra data was acquired using a JEOL AccuTOF-CS using ESI-TOF. All synthesis and characterization can be found in the Supplemental information.

**Laser Flash Photolysis:** Laser flash photolysis experiments were performed using a Nd:YAG laser pump beam source with a Continuum Surelite II-10 capable of 266, 532, or 355 nm pulses between 4-6 ns. A LeCroy 350 MHz digital oscilloscope was used to observe all waveforms. Samples were prepared so that their relative absorbance was between 0.75 and 1.5 at the excitation wavelength, 355 nm. The probe beam was a 350 W Xenon arc lamp. The samples were loaded into a 1 cm quartz cuvette and  $\text{N}_2$  was purged for 10 minutes in the solution and an additional 5 minutes in the headspace. Samples were flowed continuously thorough out the experiment to avoid buildup of photoproducts.

**Polymerization Procedure:** In a 3.5 dr vial the appropriate amount of AQ-1 in DMSO and 13.1 mg (46.9 mmol) of CPADB was added and the solution was sonicated in the absence of light until everything dissolved. Methyl methacrylate (MMA), 1 mL, was added and the mixture was thoroughly mixed. If polymerizing in the presence of air, the cap was sealed and the vial was photolyzed in the Rayonet photoreactor (419 nm broadband irradiation) for the appropriate amount of time. If polymerizing under an inert atmosphere, the vial was sealed with a septum and purged with  $\text{N}_2$  for 10 minutes in the solution and

an additional 5 minutes in the headspace. Unless otherwise noted, the conversion was measured by taking a small ( $\approx 10 \mu\text{L}$ ) amount of the mixture and adding it to 0.5 mL of  $\text{CD}_3\text{CN}$  for  $^1\text{H}$  NMR. The amount of monomer loss was measured using the signal of DMSO, 2.5 ppm, as the internal standard and comparing it to the loss of signal at 3.7 ppm corresponding to MMA.

## RESULTS AND DISCUSSION

The photocatalyst (AQ-1) which was synthesized according to previously published methods,<sup>34</sup> has an absorption tail that extends out to 440 nm allowing for the polymerizations to be carried out with visible light (Figure S2). Polymerization reactions were performed with 4-cyanopentanoic acid dithiobenzoate (CPADB) as a chain transfer agent due to its photolytic stability under visible light irradiation, and AQ-1 in DMSO was used as the photoinitiator.

### Polymerization

Unless otherwise noted, polymerizations were carried out at 419 nm under broadband irradiation in a 35 W, 16 bulb Rayonet photoreactor with an operating temperature of 35°C. Photolysis of AQ-1 in a mixture of DMSO/MMA resulted in polymer formation (Table 1, Entry 1). This demonstrates that photolysis of AQ-1 in DMSO results in the formation of initiating radicals in the absence of a co-sensitizer. The polymerization process was able to be controlled with the addition of CPADB resulting in low polydispersity and good agreement between predicted and measured molecular weights (Table 1, Entries 4-12.). The presence of the dithiobenzoate end group was confirmed by  $^1\text{H}$  NMR of the products, along with detection of its characteristic UV/vis absorption at 300 nm (Figures S9, S14). Although purging the solution with nitrogen prior to photolysis resulted in slightly higher conversions than those carried out in air, the effect was minimal (Table S1).

<Table 1>

To assess the feasibility of the photocatalyst in low concentrations, polymerizations were carried out using sub-mM amounts of AQ-1 (Table 1, Entries 5-10. Fig. 2). Encouragingly, all experiments showed an increase in conversion and molecular weight relative to background

polymerization while maintaining control over the polymerization process. Examples where the solution was left unexposed to light resulted in no conversion, and although control experiments confirm the polymerization to be photocatalytically initiated, some background photolysis of the CTA is observed (Table 1, Entries 2-3). One possible explanation for the observed background polymerization is due to contributions from a photoiniferter mechanism involving the UV edge of the broadband emission of 419 nm bulbs (Figure S2).

<Figure 2>

Increasing photolysis time shows a general increase in conversion and molecular weight of the formed polymers, but also leads to larger disagreements between observed and theoretical molecular weights (Table 1, Entries 9-10). This suggests that some degradation of the end group occurs with prolonged photolysis which is consistent with both the background polymerization experiments and has been observed previously using UV irradiation.<sup>13, 14</sup>

The polymerization process was applied to multiple methacrylate monomers (Table S2). Well-defined polymers with good agreement between predicted and measured molecular weights were achieved for both MAA and GMA, but DMAEMA showed significant degradation of the CTA and, consequently, poor control over the molecular weight. As shown in Fig. 1, DMAEMA has an alkyl amino substituent at one of the terminal positions. Anthraquinones are well known to act as excited state oxidants of alkyl amines and substituted amines are commonly used as sacrificial electron donors in photoinduced electron transfer process.<sup>37</sup> The reaction of the excited state AQ-1 with DMAEMA likely results in unwanted radical formation and redox process which, in turn, may be responsible for the poor polymer properties.

Figure 3 illustrates ‘On’ / ‘Off’ experiments that were performed to demonstrate the temporal control over the reaction process. In the absence of light, no conversion is observed, while during photolysis, a noticeable increase in the conversion of monomer is seen. Additionally, a polymerization was carried out in which a sample was photolyzed for a short period of time followed by an extended incubation period in the dark (Table S2, Entry 2). After the incubation period, low amounts of conversion were measured which indicates that radical species formed are quickly quenched and do

not propagate extensively in the absence of light. This further demonstrates the necessity of light for continuous formation of initiating radicals and rules out “dark” polymerization that have been reported previously.<sup>42</sup>

<Figure 3>

Photopolymerization reactions were also carried out in different solvents to assess the viability of the proposed mechanism and examine the versatility of this approach. Polymerization was observed irrespective of the solvent used, but with DMSO having the highest conversion and  $M_n$  while still maintaining a controlled process (Table 2, Entry 1). Other solvents studied all showed much lower conversion suggesting that AQ-1 is unable to efficiently generate initiating radicals and the polymerization is dominated by an iniferter mechanism. Interestingly, methanol, which is known to be a weak H-atom donor and has been shown to serve as a H-atom donor in the photochemical production of semiquinones, showed very poor control over the polymerization process and very low conversion which indicates that any semiquinone formed during photolysis is not beneficial to the polymerization process (Table 2, Entry 3).

<Table 2>

### Mechanistic Analysis

The feasibility of excited-state electron transfer can be estimated using the Rehm-Weller equation and, using this relationship, electron transfer from DMSO to AQ-1<sup>3\*</sup> is expected to be exergonic by ca. 12 kcal•mol<sup>-1</sup> (Supplemental Information, Eq 1-3). To support this, pulsed photolysis (354.7 nm, 10 mJ, 5-7 ns) of AQ-1 in DMSO was performed (Fig. 4). Under an atmosphere of either N<sub>2</sub> or air, an intermediate is formed with absorption bands at 490 and 620 nm and a lifetime of ca. 0.5  $\mu$ s. This early species is assigned to AQ-1<sup>3\*</sup> on the basis of its resemblance to triplet-state spectra of structurally similar anthraquinone derivatives, reactivity towards molecular oxygen (Figure S3), and similarity to the spectra from pulsed photolysis of AQ-1 in a non-reactive solvent, acetonitrile (Figure S4).<sup>37</sup> Following the decay of the triplet, a longer-lived species is formed with a peak at 550 nm after ca. 1  $\mu$ s which is quenched by air (Figure S5). This longer-lived signal is assigned to the anion radical



(AQ-1<sup>-•</sup>) formed after the triplet oxidation of DMSO.<sup>37</sup> This signal is consistent with the anion radical formed from pulsed photolysis of AQ-1 in acetonitrile with 1,4-diazabicyclo[2.2.2]octane (DABCO), a ground state electron donor (Fig. 4C > 700 ns). The results from pulsed photolysis demonstrate that photolysis of AQ-1 in DMSO results in the formation AQ-1<sup>-•</sup> from one-electron oxidation of DMSO as predicted by the Rehm-Weller equation.

<Figure 4>

One commonly invoked initiation mechanism in photocatalytic RAFT reactions is electron transfer from the reduced photocatalyst to the CTA. The effect of CPADB on AQ-1<sup>-•</sup> was explored. The latter was generated by pulsed photolysis of AQ-1 in methanol using triethylamine (TEA) as an electron donor (Figure S6). Kinetic traces showing the decay of AQ-1<sup>-•</sup> in the presence of CPADB are provided in Fig. 5. No noticeable change in the decay rate for the AQ-1<sup>-•</sup> is observed, however, the magnitude of the initial signal decreases with increasing concentrations of CPADB (Fig. 5). Stern–Völmer analysis (Fig. 6) demonstrates that CPADB quenches AQ-1<sup>3\*</sup> at the diffusion limit by averaging the signal corresponding to AQ-1<sup>-•</sup> over 1 μs (blue area, Fig. 5) and plotting the change in signal with respect to the concentration of quencher. A linear relationship was observed which is indicative of energy transfer from AQ-1<sup>3\*</sup> to CPADB which agrees with previous work in a non-reactive solvent demonstrating AQ-1<sup>3\*</sup> energy transfer to CPADB with a rate of 3.4x10<sup>9</sup> s<sup>-1</sup>.<sup>21</sup>

<Figure 5>

<Figure 6>

The pulsed photolysis experiments help to explain the mechanism of initiation. Namely, AQ-1<sup>3\*</sup> oxidizes DMSO to form AQ-1<sup>-•</sup> and the corresponding DMSO cation radical. Although CPADB quenches AQ-1<sup>3\*</sup> as well, significant contribution to the polymerization process of a PET-Energy Transfer-RAFT pathway can be ruled out given the high concentration of DMSO, concentration of air present in the polymerization procedure with respect to the CTA, and previous work demonstrating that triplet energy transfer to the first excited triplet of CPADB does not result in significant C-S bond dissociation.<sup>21</sup> Additionally, the lifetime of AQ-1<sup>-•</sup> is independent of the amount of CPADB present

which shows that the reduced quinone is not responsible for the activation of the chain transfer agent leading to polymerization. Thus, we can exclude contribution due to a PET-RAFT process in which  $AQ-1^{-\bullet}$  acts to reduce the CTA.

#### <Scheme 2>

Chemical trapping experiments support the formation of methyl radicals. As shown in Scheme 2, the methyl radical is expected to react with CPADB forming the methyl-adduct, and an alkyl radical. For these experiments AQ-1 was photolyzed in DMSO in the presence of CPADB, in the absence of monomer and the photoproduct was analyzed by MS. After photolysis, a mass corresponding to the methyl ester was found which matched an independently synthesized standard (Figures S17, 18).

In addition to generating methyl radicals, the proposed mechanism also suggests formation of sulfinic acid. This is supported by photolysis of AQ-1 in DMSO followed by detection of acid using malachite green carbinol base as a pH indicator (Figures S7, 8). With increasing photolysis time, the yield of acid increased accordingly. Control experiments conducted in the absence of AQ-1 or in the absence of irradiation resulted in no acid detection, providing further mechanistic support. Interestingly, sulfinic acid may also be a source of reactive alkyl radicals resulting from oxidation, but this possibility was not investigated in the current study.<sup>43</sup>

#### <Scheme 3>

The proposed mechanism of contributions to the initiation of polymerization from photo-oxidation of DMSO is shown in Scheme 3. The photosensitizer, AQ-1, absorbs a photon and, after intersystem crossing, forms its triplet state. The latter oxidizes DMSO leading to the formation of the anthraquinone anion radical, and a DMSO cation radical. The cation radical is trapped by latent water to yield sulfinic acid and a methyl radical. The methyl radical can combine with monomer to initiate polymerization and enter into the RAFT process. In the presence of air,  $AQ-1^{-\bullet}$  can react with molecular oxygen to regenerate AQ-1.

## CONCLUSION

The solvent plays a crucial role in any reaction mechanism. This study demonstrates that photochemical oxidation of DMSO can be used to generate radicals and prepare methacrylate polymers with high conversions and a narrow PDI. Through the use of a suitably substituted anthraquinone derivative, these reactions can be carried out with visible light and in the presence of air. Pulsed photolysis results and chemical trapping experiments support contributions to the initiation proposed in Scheme 3 wherein the DMSO cation radical reacts with water to produce sulfinic acid along with reactive methyl radicals. Given that DMSO is a widely used solvent for photocatalytic RAFT polymerizations, and many of the photocatalysts are highly effective excited-state oxidants, the role of the solvent must be more carefully considered when discussing the mechanisms involved in photo-RAFT processes.

**ACKNOWLEDGEMENTS:** This work has been supported in part by the National Science Foundation (CHE-1112018).

## SUPPORTING INFORMATION

Additional supporting information may be found online in the Supporting Information section at the end of the article:

**Figure S1.** Synthesis of methyl benzodithioate.

**Figure S2.** Normalized absorption spectra of AQ-1 and CPADB in MeCN. Normalized emission spectrum of the 419 nm bulbs from the Rayonet photoreactor.

**Figure S3.** *Left:* Waveforms from pulsed photolysis of AQ-1 in DMSO 640 nm. The lifetime of the signal corresponding to AQ-1<sup>3\*</sup> is affected little by the presence of air suggesting efficient quenching of AQ-1<sup>3\*</sup> by DMSO. *Right:* Waveforms from pulsed photolysis of AQ-1 in DMSO 550 nm. The lifetime of the signal corresponding to AQ-1<sup>•</sup>, on the other hand, is significantly decreased in air due to quenching of AQ-1<sup>•</sup> by molecular oxygen. On the other hand, at early times (< 0.5 μs), where the signal for AQ-1<sup>3\*</sup> dominates, little effect is seen.

**Figure S4.** *Left:* Transient absorption spectrum of AQ-1 in MeCN under N<sub>2</sub>. The peaks corresponding to AQ-1<sup>3\*</sup> are seen at 490 and 630 nm. *Right:* Waveforms showing quenching of AQ-1<sup>3\*</sup> in air (orange) at 490 nm.

**Figure S5.** Waveforms from transient absorption spectrum of AQ-1 in MeCN with 2 mM DABCO under N<sub>2</sub> at 550 nm. Waveforms show the decay of the anion radical of AQ-1 in the presence of air (orange).

**Figure S6.** *Left:* Transient absorption spectrum of AQ-1 in MeOH with 25 mM TEA under N<sub>2</sub>. The sample was continuously flowed to avoid the buildup of photoproducts. A very long-lived peak at 490 nm is assigned to AQ-1<sup>•-</sup>. Also notable is the semiquinone which can be seen at 410 nm. *Right:* Waveforms illustrating the quenching of AQ-1<sup>•-</sup> by molecular oxygen.

**Figure S7.** Monitoring formation of acid over time from photolysis of AQ-1 in DMSO using malachite green carbinol base as a pH indicator. Blue: 370 nm irradiation of AQ-1 in DMSO; Orange: 370 nm irradiation of DMSO in the absence of AQ-1; Gray: AQ-1 in DMSO without irradiation.

**Figure S8.** Monitoring formation of acid over time from photolysis of AQ-1 in DMSO using malachite green carbinol base as a pH indicator. Acid formation is detected by the growth of the band at 633 nm.

**Table S1.** RAFT Polymerization of MMA with AQ-1 in DMSO under Nitrogen

**Table S2.** Polymerization scope and limitations in Air

**Figure S9.** UV/Vis spectra of Table 1, entry 11.

**Figure 10.** UV/Vis spectra of Table 1, entry 4.

**Figure S11.** <sup>1</sup>H NMR of Table 1, entry 11.

**Figure S12.** <sup>1</sup>H NMR of Table 1, entry 4.

**Figure S13.** <sup>1</sup>H NMR of Table S2, entry 3.

**Figure S14.** <sup>1</sup>H NMR of Table S2, entry 4.

**Figure S15.** <sup>1</sup>H NMR of methyl benzodithioate.

**Figure S16.** <sup>13</sup>C NMR of methyl benzodithioate.

**Figure S17.** Mass Spec (DART-) of methyl benzodithioate in CD<sub>3</sub>CN.

**Figure S18.** Mass Spec (DART-) showing formation of methyl benzodithioate from photolysis of AQ-1 and CPADB in DMSO. The peaks corresponding to the photoproduct are shown starting at M/Z

## REFERENCES

- (1) Hill, M. R., Carmean, R. N., Sumerlin, B. S. (2015) Expanding the Scope of RAFT Polymerization: Recent Advances and New Horizons. *Macromolecules* **48**, 5459–5469.
- (2) Chen, M., Zhong, M., Johnson, J. A. (2016) Light-Controlled Radical Polymerization: Mechanisms, Methods, and Applications. *Chem. Rev.*, **116**, 10167–10211.
- (3) Pan, X., Tasdelen, M. A., Laun, J., Junkers, T., Yagci, Y., Matyjaszewski, K. (2016) Photomediated Controlled Radical Polymerization. *Prog. Polym. Sci.* **62**, 73–125.
- (4) McKenzie, T. G., Fu, Q., Uchiyama, M., Satoh, K., Xu, J., Boyer, C., Kamigaito, M., Qiao, G. (2016) Beyond Traditional RAFT: Alternative Activation of Thiocarbonylthio Compounds for Controlled Polymerization. *Adv. Sci.* **3**, 1500394.

- (5) Shanmugam, S., Xu, J., Boyer, C. (2017) Photocontrolled Living Polymerization Systems with Reversible Deactivations through Electron and Energy Transfer. *Macromol. Rapid Commun.* **38**, 1700143.
- (6) Phommalsack-Lovan, J., Chu, Y., Boyer, C., Xu, J. (2018) PET-RAFT Polymerisation: Towards Green and Precision Polymer Manufacturing. *Chem. Commun.* **54**, 6591– 6606.
- (7) McKenzie, T. G., Fu, Q., Wong, E. H. H., Dunstan, D. E., Qiao, G. G. (2015) Visible Light Mediated Controlled Radical Polymerization in the Absence of Exogenous Radical Sources or Catalysts. *Macromolecules* **48**, 3864–3872.
- (8) Otsu, T. (2000) Iniferter Concept and Living Radical Polymerization. *J. Polym. Sci. Part A Polym. Chem.* **38**, 2121–2136.
- (9) Khan, M. Y., Cho, M. S., Kwark, Y. J. (2014) Dual Roles of a Xanthate as a Radical Source and Chain Transfer Agent in the Photoinitiated RAFT Polymerization of Vinyl Acetate. *Macromolecules* **47**, 1929–1934.
- (10) Shanmugam, S., Cuthbert, J., Kowalewski, T., Boyer, C., Matyjaszewski, K. (2018) Catalyst-Free Selective Photoactivation of RAFT Polymerization: A Facile Route for Preparation of Comblike and Bottlebrush Polymers. *Macromolecules* **51**, 7776–7784.
- (11) Quinn, J. F., Barner, L., Barner-Kowollik, C., Rizzardo, E., Davis, T. P. (2002) Reversible Addition - Fragmentation Chain Transfer Polymerization Initiated with Ultraviolet Radiation. *Macromolecules* **35**, 7620–7627.
- (12) You, Y., Hong, C., Bai, R., Pan, C., Wang, J. (2002) Photo-Initiated Living Free Radical Polymerization in the Presence of Dibenzyl Trithiocarbonate. *Macromol. Chem. Phys.* **203**, 477–483.
- (13) Lu, L., Zhang, H., Yang, N., Cai, Y. (2006) Toward Rapid and Well-Controlled Ambient Temperature RAFT Polymerization under UV–Vis Radiation: Effect of Radiation Wave Range. *Macromolecules* **39**, 3770–3776.

- (14) Quinn, J. F., Barner, L., Barner-Kowollik, C., Rizzardo, E., Davis, T. P. (2002) Reversible Addition - Fragmentation Chain Transfer Polymerization Initiated with Ultraviolet Radiation. *Macromolecules* **35**, 7620–7627.
- (15) Carmean, R. N., Becker, T. E., Sims, M. B., Sumerlin, B. S. (2017) Ultra-High Molecular Weights via Aqueous Reversible-Deactivation Radical Polymerization. *Chem.* **2**, 93– 101.
- (16) Xu, J., Jung, K., Boyer, C. (2014) Oxygen Tolerance Study of Photoinduced Electron Transfer–Reversible Addition–Fragmentation Chain Transfer (PET-RAFT) Polymerization Mediated by Ru(Bpy)<sub>3</sub>Cl<sub>2</sub>. *Macromolecules* **47**, 4217–4229.
- (17) Xu, J., Jung, K., Atme, A., Shanmugam, S., Boyer, C. (2014) A Robust and Versatile Photoinduced Living Polymerization of Conjugated and Unconjugated Monomers and Its Oxygen Tolerance. *J. Am. Chem. Soc.* **136**, 5508–5519.
- (18) Tu, K., Xu, T., Zhang, L., Cheng, Z., Zhu, X. (2017) Visible Light-Induced PET-RAFT Polymerization of Methacrylates with Novel Organic Photocatalysts. *RSC Adv.* **7**, 24040–24045.
- (19) Niu, J., Page, Z. A., Dolinski, N. D., Anastasaki, A., Hsueh, A. T., Soh, H. T., Hawker, C. J. (2017) Rapid Visible Light-Mediated Controlled Aqueous Polymerization with In Situ Monitoring. *ACS Macro Lett.* **6**, 1109–1113.
- (20) Shanmugam, S., Xu, J., Boyer, C. (2015) Exploiting Metalloporphyrins for Selective Living Radical Polymerization Tunable over Visible Wavelengths. *J. Am. Chem. Soc.* **137**, 9174–9185.
- (21) Thum, M. D., Wolf, S., Falvey, D. E. (2020) State-Dependent Photochemical and Photophysical Behavior of Dithiolate Ester and Trithiocarbonate Reversible Addition–Fragmentation Chain Transfer Polymerization Agents. *J. Phys. Chem. A* **124**, 4211– 4222.
- (22) Allegranza, M. L., Konkolewicz, D. (2021) PET-RAFT Polymerization: Mechanistic Perspectives for Future Materials *ACS Macro Lett.* **10**, 433–446.

- (23) Corrigan, N., Xu, J., Boyer, C., Allonas, X. (2019) Exploration of the PET-RAFT Initiation Mechanism for Two Commonly Used Photocatalysts. *ChemPhotoChem*. **3**, 1193– 1199.
- (24) Kottisch, V., Michaudel, Q., Fors, B. P. (2017) Photocontrolled Interconversion of Cationic and Radical Polymerizations. *J. Am. Chem. Soc.* **139**, 10665–10668.
- (25) Xu, J., Shanmugam, S., Duong, H. T., Boyer, C. (2015) Organo-Photocatalysts for Photoinduced Electron Transfer-Reversible Addition–Fragmentation Chain Transfer (PET-RAFT) Polymerization. *Polym. Chem.* **6**, 5615-5624.
- (26) Michaudel, Q., Chauviré, T., Kottisch, V., Supej, M. J., Stawiasz, K. J., Shen, L., Zipfel, W. R., Abruña, H. D., Freed, J. H., Fors, B. P. (2017) Mechanistic Insight into the Photocontrolled Cationic Polymerization of Vinyl Ethers. *J. Am. Chem. Soc.* **139**, 15530–15538.
- (27) Corrigan, N., Xu, J., Boyer, C. A (2016) Photoinitiation System for Conventional and Controlled Radical Polymerization at Visible and NIR Wavelengths. *Macromolecules* **49**, 3274–3285.
- (28) Evoniuk, C. J., Gomes, G., Hill, S. P., Fujita, S., Hanson, K., Alabugin, I. V. (2017) Coupling N–H Deprotonation, C–H Activation, and Oxidation: Metal-Free C(sp<sup>3</sup>)–H Aminations with Unprotected Anilines *J. Am. Chem. Soc.* **139**, 16210–16221.
- (29) Kishore, K., Asmus, K. D. (1989) Radical Cations from One-Electron Oxidation of Aliphatic Sulfoxides in Aqueous Solution. A Radiation Chemical Study. *J. Chem. Soc. Perkin Trans. 2.* **12**, 2079-2084.
- (30) Gollnick, K., Stracke, H. U. (2008) Direct and Sensitized Photolysis of Dimethyl Sulphoxide in Solution. *Pure Appl. Chem.* **33**, 217–246.
- (31) Garg, S., Rose, A. L., Waite, T. D. (2007) Production of Reactive Oxygen Species on Photolysis of Dilute Aqueous Quinone Solutions. *Photochem. Photobiol.* **83**, 904–913.
- (32) Veltwisch, D., Janata, E., Asmus, K. D. (1980) Primary Processes in the Reaction of Hydroxyl Radicals with Sulfoxides. *J. Chem. Soc., Perkin Trans. 2.* **1**, 146–153.



- (33) Crean, C., Geacintov, N. E., Shafirovich, V. (2009) Methylation of 2'-Deoxyguanosine by a Free Radical Mechanism. *J. Phys. Chem. B* **113**, 12773–12781.
- (34) Thum, M. D., Falvey, D. E. (2018) Photoreleasable Protecting Groups Triggered by Sequential Two-Photon Absorption of Visible Light: Release of Carboxylic Acids from a Linked Anthraquinone- N -Alkylpicolinium Ester Molecule. *J. Phys. Chem. A* **122**, 3204–3210.
- (35) Ly, D., Kan, Y., Armitage, B., Schuster, G. B. (1996) Cleavage of DNA by Irradiation of Substituted Anthraquinones: Intercalation Promotes Electron Transfer and Efficient Reaction at GG Steps. *J. Am. Chem. Soc.* **118**, 8747–8748.
- (36) Breslin, D. T., Schuster, G. B. (1996) Anthraquinone Photoreductases: Mechanisms for GG-Selective and Nonselective Cleavage of Double-Stranded DNA. *J. Am. Chem. Soc.* **118**, 2311–2319.
- (37) Görner, H. (2003) Photoreduction of 9,10-Anthraquinone Derivatives: Transient Spectroscopy and Effects of Alcohols and Amines on Reactivity in Solution. *Photochem. Photobiol.* **77**, 171–179.
- (38) Bardagi, J. I., Ghosh, I., Schmalzbauer, M., Ghosh, T., König, B. (2018) Anthraquinones as Photoredox Catalysts for the Reductive Activation of Aryl Halides. *European J. Org. Chem.* **1**, 34–40.
- (39) Kuss-Petermann, M., Wenger, O. S. (2016) Electron Transfer Rate Maxima at Large Donor–Acceptor Distances. *J. Am. Chem. Soc.* **138**, 1349–1358.
- (40) Kuss-Petermann, M., Oraziotti, M., Neuburger, M., Hamm, P., Wenger, O. S. (2017) Intramolecular Light-Driven Accumulation of Reduction Equivalents by Proton-Coupled Electron Transfer. *J. Am. Chem. Soc.* **139**, 5225–5232.
- (41) Görner, H. (2005) Photoreactions of P-Quinones with Dimethyl Sulfide and Dimethyl Sulfoxide in Aqueous Acetonitrile. *Photochem. Photobiol.* **82**, 71–77.
- (42) Shanmugam, S., Xu, J., Boyer, C. (2017) Photoinduced Oxygen Reduction for Dark Polymerization. *Macromolecules* **50**, 1832–1846.

(43) Gomes, G.; Wimmer, A.; Smith, J.; König, B.; Alabugin, I.V. (2019) CO<sub>2</sub> or SO<sub>2</sub>: Should It Stay, or Should It Go? *J. Org. Chem.* **84**, 6232-6243.

## FIGURE CAPTIONS

**Scheme 1.** Photo-oxidation of DMSO leads to the formation of reactive methyl radicals.

**Figure 1.** Compounds used in this study. The synthesis of AQ-1 has been reported previously.<sup>34</sup> MAA, DMAEMA, GMA, stand for methacrylic acid, N,N-diaminoethyl methacralate, glycidyl methacralate, respectively.

**Figure 2.** GPC traces showing narrow molecular weight distributions and an increasing in the Mn with increasing concentrations of photoinitiator used.

**Figure 3.** Reaction process was monitored by <sup>1</sup>H NMR during polymerization. During photolysis (white regions) noticeable amounts of monomer were consumed while, in the dark (grey regions), no significant change was noted. Conversions were estimated to  $\pm 2\%$ . The seeming decrease monomer conversion in dark periods shown in Fig. 3 is likely due to errors inherent in the conversion measurement.

**Figure 4.** Transient absorption spectrum of AQ-1 in DMSO in air (A) and under N<sub>2</sub> (B). Transient absorption spectrum of AQ-1 in MeCN with 2 mM DABCO.

**Figure 5.** Waveforms at 490 nm of AQ-1<sup>-•</sup> generated by pulsed photolysis of AQ-1 in MeOH with TEA under N<sub>2</sub>. The addition of increasing concentrations of CPADB result a smaller magnitude for signal for AQ-1<sup>-•</sup> due to competitive quenching between CPADB and TEA.

**Figure 6.** Stern Völmer analysis. The change in  $\Delta O.D.$  averaged over 1  $\mu s$  is plotted with respect to the concentration of CPADB. The  $\tau$  is estimated from the waveforms in Fig. 6 to calculate the  $k_q$  from the slope of a linear fit to the data.

**Scheme 2.** Formation of methyl benzodithioate and sulfinic acid from photolysis of AQ-1 in DMSO.

**Scheme 3.** Mechanism for the photo-oxidation of DMSO by AQ-1 followed by radical formation and subsequent RAFT polymerization.

Table 1: RAFT Polymerization with AQ-1 in a DMSO/Monomer mixture in the presence of Air

Entry	M/CTA	[AQ-1] <sup>a</sup> , equiv.	Photolysis Time, hrs	M <sub>n, GPC</sub> <sup>b</sup>	M <sub>n, theo</sub> <sup>c</sup>	PDI	Conv. <sup>d</sup>
1	0	0.1	4	42.1k	-	1.61	21%
2	200	0	8	7.6k	5.6k	1.03	26%
3	200	0	16	9.8k	12.2k	1.05	59%
4	200	0.1	DARK	-	-	-	0%
5	200	0.01	8	10.8k	7.8k	1.16	37%
6	200	0.02	8	8.7k	9.5k	1.06	45%
7	200	0.03	8	8.7k	10.5k	1.02	50%
8	200	0.04	8	9.1k	10.9k	1.03	52%
9	200	0.05	8	9.9k	12.3k	1.14	59%
10	200	0.05	16	13.1k	19.2k	1.23	93%
11	200	0.1	8	9.1k	9.5k	1.06	45%
12	200	0.1	16	10.1k	15.7k	1.03	76%

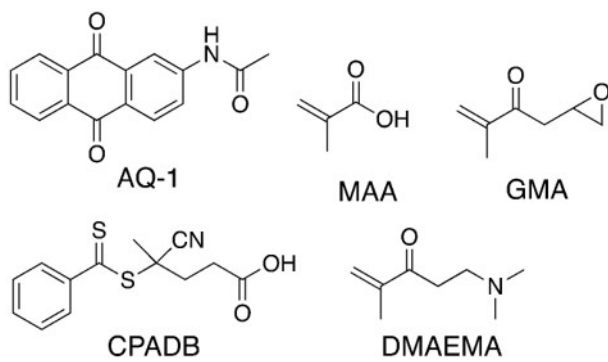
<sup>a</sup> Relative to the amount of CTA-1. <sup>b</sup> Measured by GPC using THF as the solvent and calibration using polystyrene standards.

<sup>c</sup> Calculated according to the following equation:  $M_{n, theo} = [M]_0/[CTA]_0 \cdot MW_M \cdot conv. + MW_{CTA}$ . Where  $[M]_0$ ,  $[CTA]_0$ ,  $MW_M$ , conv.,  $MW_{CTA}$ , correspond to initial concentration of monomer, M, the initial concentration of RAFT agent, the molecular weight of the monomer, the fraction of monomer converted into polymer and the molecular weight of the RAFT agent respectively. <sup>d</sup> Determined using <sup>1</sup>H NMR.

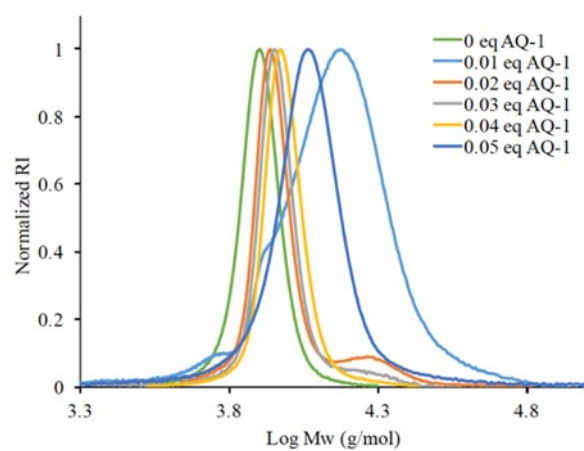
Table 2: Solvent dependence on the RAFT polymerization of MMA with AQ-1

Entry	CTA/I	[AQ-1] <sup>a</sup> , equiv.	Solvent	Photolysis Time, hrs	M <sub>n</sub> <sup>b</sup>	PDI <sup>b</sup>	Conv. <sup>c</sup>
1	200	0.05	DMSO	16	13.1k	1.23	93%
2	200	0.05	Toluene	16	11.0k	1.30	34%
3	200	0.05	MeOH	16	8.4k	2.09	21%
4	200	0.05	MeCN	16	11.9k	1.12	40%
5	200	0.05	THF	16	9.0k	1.06	32%

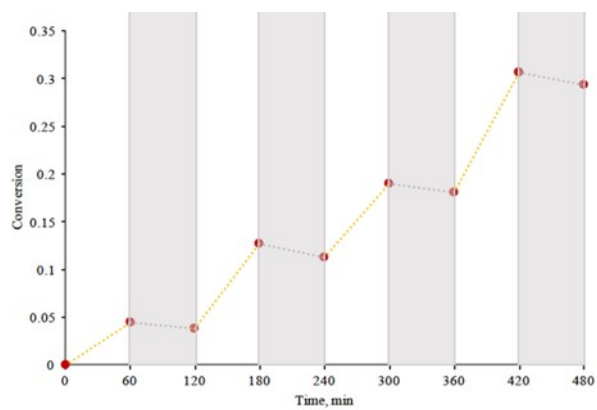
Photolysis at 419 nm. <sup>a</sup> Relative to the amount of CTA-1. <sup>b</sup> Measured by GPC using THF as the solvent and calibration using polystyrene standards. <sup>c</sup> Determined using <sup>1</sup>H NMR.



php\_13468\_f1.jpg

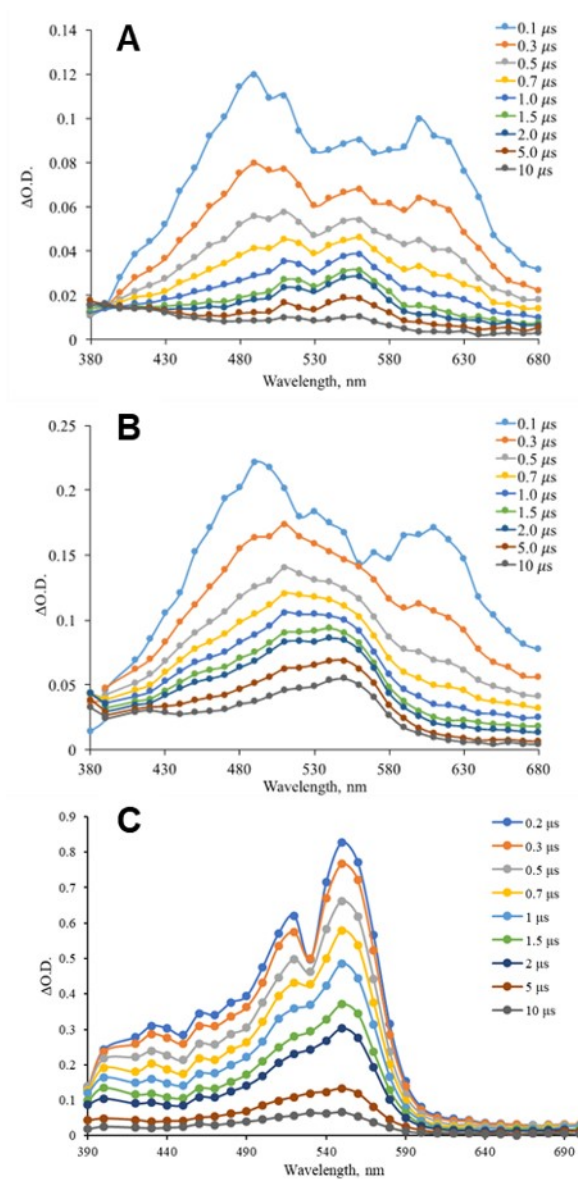


php\_13468\_f2.jpg

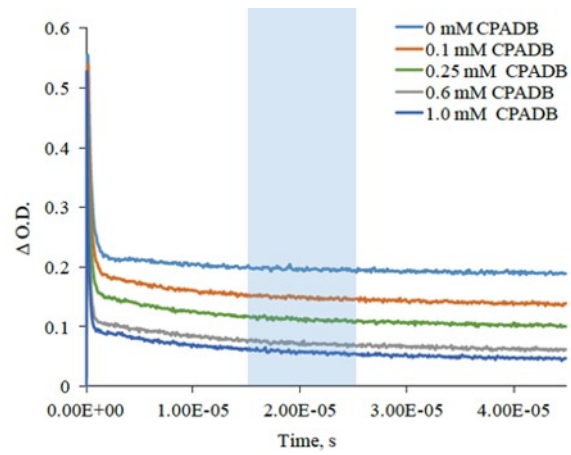


php\_13468\_f3.jpg

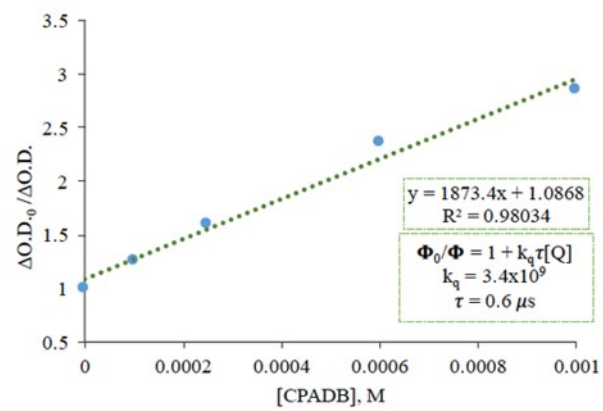




php\_13468\_f4.jpg



php\_13468\_f5.jpg



php\_13468\_f6.jpg

